Separation Science and Technology
Publication details, including instructions for authors and subscription information:
http://www.informaworld.com/smpp/title~content=t713708471

Settling behavior of specific acrylic particles in Bis-GMA based reactive slurries

P. I. Dolez[a]; A. Goff[a]; B. J. Love[a]
[a] Materials Science and Engineering Department, 213 Holden Hall, Virginia Polytechnic Institute and State University, Blacksburg, VA, U.S.A.

Online publication date: 13 June 2002

To cite this Article Dolez, P. I. , Goff, A. and Love, B. J.(2002) 'Settling behavior of specific acrylic particles in Bis-GMA based reactive slurries', Separation Science and Technology, 37: 9, 2007 — 2019
To link to this Article: DOI: 10.1081/SS-120003498
URL: http://dx.doi.org/10.1081/SS-120003498

SEPARATION SCIENCE AND TECHNOLOGY, 37(9), 2007–2019 (2002)

SETTLING BEHAVIOR OF SPECIFIC ACRYLIC PARTICLES IN BIS-GMA BASED REACTIVE SLURRIES

P. I. Dolez,* A. Goff, and B. J. Love

Virginia Polytechnic Institute and State University,
Materials Science and Engineering Department,
213 Holden Hall, Blacksburg, VA 24061

ABSTRACT

Sedimentation is a limiting factor for the shelf life of filled paints and adhesive resins, and requires consideration when optimizing a resin's formulation for an end application. Static settling experiments have been performed using a bis-GMA-based photocurable resin system by varying some characteristics of the filler particles (size and composition) and of the resin (viscosity and composition). The recorded batch settling curves, mudline height vs. time, displayed the standard sedimentation shape. In particular, the mudline movement rate was constant in the initial period of sedimentation. The variations of this constant mudline velocity as a function of the settling conditions has been compared to sedimentation model predictions. A close correspondence has been obtained between the data and a model describing the sedimentation behavior of non-aggregated rigid spheres at high concentration in the Stokes regime. In particular, the constant mudline velocity is proportional to the square of the

*Corresponding author. Fax: (540) 231-3554; E-mail: pdolez@vt.edu

particle diameter. This result can be used as a way to limit the settling phenomenon in filled resin systems, by choosing a particle diameter as small as possible. As a validation of this result, no visually observable settling was seen in 50%-filled resin systems for a period more than 4 months at room temperature using 5.1-μm poly(methyl methacrylate-*co*-ethylene glycol dimethacrylate) particles as filler.

Key Words: Particle settling; Polymer slurry; Sedimentation model

INTRODUCTION

Sedimentation is a long-known phenomenon. While it is decried for its damaging effects, for example in clogging harbors and other marine structures with sand (1), it is also a very cost-effective process for thickening metallurgical and chemical slurries (2), and in waste treatment facilities (3). Some sedimentation models have been developed since 1912 (2). The goal was to find a relationship between the results of settling tests done on a small scale in the laboratory, and the design parameters of the real settling device, or thickener, in particular its size.

In the field of biomaterials, the concerns about settling are concomitant with the use of filler particles as a way to improve the properties of structural polymers. For example, the addition of different sorts of filler particles to a mixture of two acrylic monomers, bis-GMA (bis-phenol-A-dimethacrylate), and triethylene glycol dimethacrylate (TEGDMA), used in dentistry as a restorative resin, has been very successful. Properties like thermal expansion, compressive strength, and resistance to indentation for restoratives have approached those of hard tooth tissues by incorporating vinylsilane-treated silica powder into the resin (4). It has been found that, to improve fatigue resistance, 60–80% by weight of silanized quartz particles has to be added to the resin (5). And finally, the wear resistance of acrylic resins was greatly enhanced with the addition of silane-treated Sr glass particles (6).

The photocurable resin system that has been developed in our laboratory for underwater bonding applications (7) is also based on bis-GMA monomer. The second monomer used as a viscosity modifier is either TEGDMA (8) or diethylene glycol diacrylate (DEGDA) (9). In our case, the role of the filler is to modify the resin viscosity and control flow properties prior to photopolymerization.

To better identify the controlling parameters in the settling phenomenon with our resin system, we have performed batch settling tests on a bis-GMA photopolymerizable matrix with two viscosity modifiers (TEGDMA and DEGDA), at three different temperatures, with three sizes of polymethyl methacrylate

(PMMA) particles and two sizes of poly(methyl methacrylate-*co*-ethylene glycol dimethacrylate) (P(MMA-*co*-EGDMA)) ones. The results are reported in this article and compared to sedimentation models developed for thickener design.

MATERIALS AND METHODS

The resin system comprises of a major monomer, bis-GMA (Cook Composite Polymers, Inc.), a viscosity modifier, TEGDMA (Aldrich) or DEGDA (Sartomer), a photoinitiator, camphorquinone, and an activator, *N*,*N*-dimethyl-*p*-toluidine. The viscosity of the unfilled resin, measured with a Brookfield viscometer, was 12.6 Poiseuille for the TEGDMA formulation at room temperature and 10.6 Poiseuille for the DEGDA mixture (1 Poiseuille = 0.1 Pa sec).

With 50% by weight of filler particles added to the resin, the viscosity can be increased to 306 Poiseuille for the TEGDMA formulation and to 288 Poiseuille for the DEGDA mixture. The 250-μm PMMA powder (Aldrich) has been sifted using 150-, 100-, 53- and 38-μm sieves. Two size distributions (50 and 8 μm) of P(MMA-*co*-EGDMA) (Aldrich) have been purchased. A Laser Scattering Particle Size Distribution Analyzer (Horiba) was used to obtain a precise measurement of the size distribution of the powder. The medians corresponding to the three PMMA powders were located at 121.5, 80.5, and 44.6 μm using a log-normal distribution. For P(MMA-*co*-EGDMA) particles, the medians were located at 40.5 and 5.1 μm. The shape of the filler particles has been investigated by SEM and is almost perfectly spherical.

Ten different slurries have been produced by mixing the TEGDMA and DEGDA resins with the five different filler powders (three particle sizes of PMMA powder, two particle sizes of P(MMA-*co*-EGDMA) powder). The cylindrical section of 10-mL pipettes (8-mm inside diameter) were used as settling vessels, their external walls being covered with dark paper to prevent any light-triggered polymerization of the resin. The resin settling behavior was studied under three temperature conditions: in an oven at 36°C, at room temperature (21°C), and in a refrigerator at 4°C. The height of the settling particle front, also called the mudline, was measured visually every day, every other day or twice a week, depending on the extent of the experiment. Data were collected more frequently at the beginning of each experiment, while, at longer times, less frequent sampling was performed.

RESULTS

Measurement of the mudline height has been taken over 3 months for all the 28 settling vessels (no DEGDA/44.6-μm PMMA samples at 4 and 36°C).

Figures 1–3 display the evolution of the mudline height during the settling process at 4, 21, and 36°C, respectively. In certain cases, the measurement was stopped when a premature polymerization was observed. This premature cure was associated with temperature-triggered polymerization of the resin and occurred within a few days for the samples settling in the oven, and after 50 days for some samples at room temperature. It can be noted that this premature cure does not seem to be connected to the particle size, but rather to the filler material: PMMA particles induced a much higher sensitivity of the resin to temperature-triggered polymerization than P(MMA-*co*-EGDMA), possibly due to a larger quantity of unreacted residual radicals left in the PMMA particles.

Another important result is that no settling has been visually observed with the 5.1-μm P(MMA-*co*-EGDMA) particles at 21 and at 4°C (Figs. 1 and 2). The room temperature data were taken over a period of about 4 months. This absence

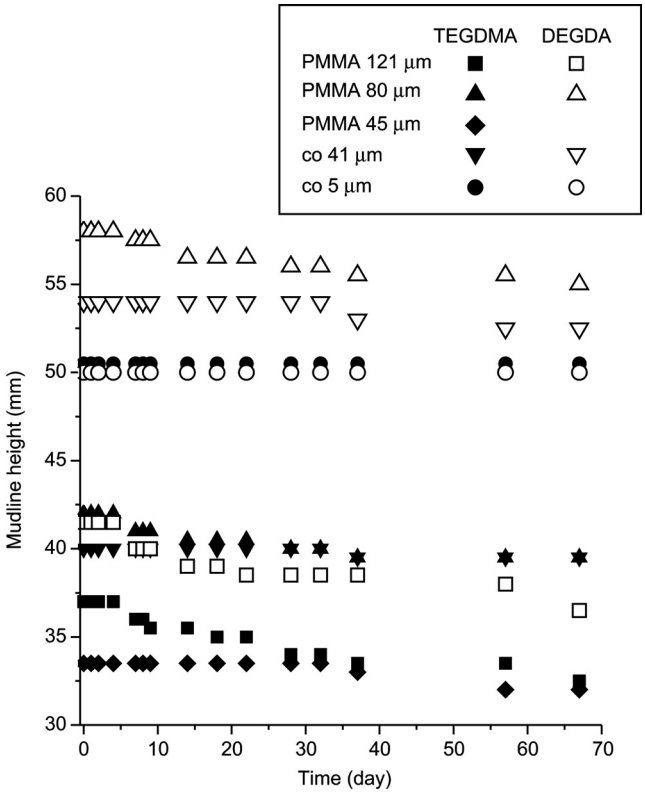

Figure 1. Settling curves for TEGDMA and DEGDA formulations at 4°C.

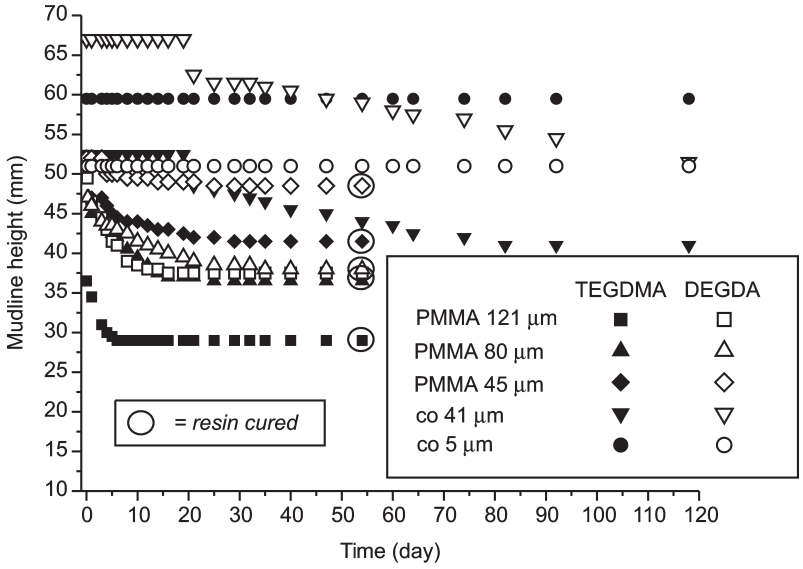

Figure 2. Settling curves for TEGDMA and DEGDA formulations at 21°C.

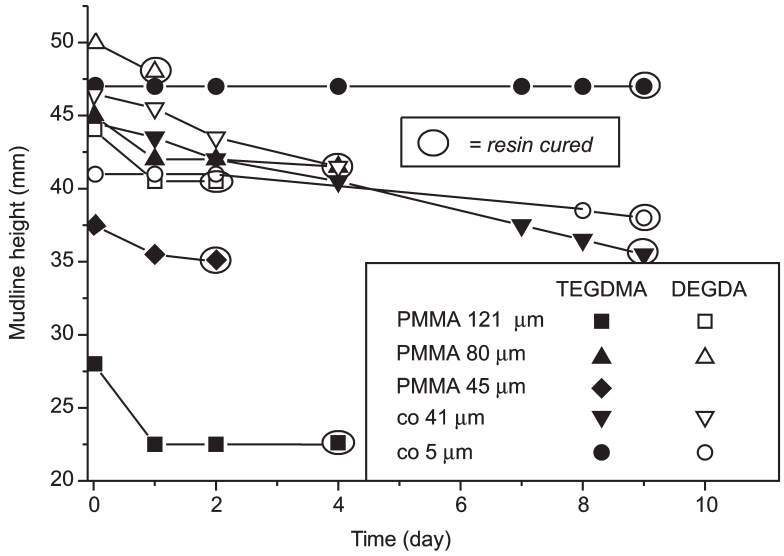

Figure 3. Settling curves for TEGDMA and DEGDA formulations at 36°C.

of observable settling shows the limitation of the visual measurement technique, which is not sensitive enough when the phenomenon occurs very slowly.

All the other settling tests visually displayed some level of sedimentation. As shown in Fig. 2 for the 40.5-μm copolymer filled DEGDA and TEGDMA resins, the onset of settling can be difficult to visually determine. The general shape of these settling curves is made of three parts. Firstly, the mudline height dropped at constant velocity. An example of this linear behavior can be seen in Fig. 3, with the 40.5-μm P(MMA-*co*-EGDMA) particles settling in TEGDMA resin. Then, the mudline height decrease slowed down and finally stabilized. Due to the temperature-triggered polymerization effect, the 36°C settling curves (Fig. 3) show only the initial step of the sedimentation process. For the 4°C data (Fig. 1), the process is so slow that, in some instances, only the first step was captured during the 70 days of recording.

THEORY OF SEDIMENTATION

As reported by Papanicolaou (3), the typical shape of batch settling curves for any stationary sedimentation test is shown in Fig. 4. The slope of the batch curve indicates the rate at which the denser particles agglomerate as a front and move towards the bottom of the vessel. The curve can be separated in three phases. In the first phase or constant regime, the solids move down as a mass at a constant rate. During the transition regime, the particle movement rate decreases, slowed down by the upward displacement of the liquid. In the last regime of consolidation, the particles accumulated at the bottom of the vessel compact under the effect of their own weight: the mudline height variation is very slow.

The most general model describes the initial part of the sedimentation process, where the settling rate is constant. It begins with a single particle falling through a fluid under the force of gravity and slowed down by the drag force exerted by the fluid. A general equation can be obtained (2,10) for the constant velocity U_T at which the spherical particle falls after the equilibrium between gravitational, buoyancy and drag forces has been reached.

$$U_T = \left[\frac{4gD^{1+n}(\rho_s - \rho)}{3b\eta^n\rho^{1-n}}\right]^{1/(2-n)}, \tag{1}$$

In Eq. (1), g is the acceleration due to gravity, D the diameter of the particle, ρ_s the fluid density, ρ the particle density, and η the fluid viscosity.

The values of the coefficients b and n depend on the flow conditions as they connect the drag coefficient C and the Reynolds number Re:$C = b/(Re)^n$. The Reynolds number is defined by $Re = D\rho U/\eta$, where U is the particle velocity. In

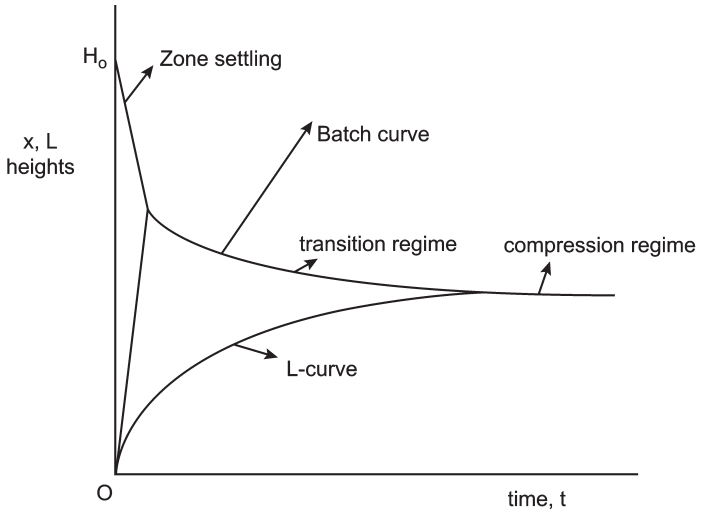

Figure 4. Typical batch settling curve, from Papanicolaou (3).

the Stokes' region, where the flow is laminar, $Re < 0.2$, n is equal to 1, and b to 24. In the transition region, $0.2 < Re < 2000$, n is equal to 0.6 and b to 18.5. Finally, in the Newton's region ($2000 < Re < 200,000$), the resistance to flow is proportional to the dynamic pressure, and the drag coefficient is constant ($n = 0$) and b is equal to 0.44.

With multiple body interactions of the particles within the fluid, the hydrodynamic interactions between the particles modify the sedimentation rate. Steinour (11) has obtained an expression for the constant settling rate of non-aggregating rigid spheres at high concentration:

$$U = U_0 \frac{\varepsilon^3}{1 - \varepsilon} f(\varepsilon), \tag{2}$$

In Eq. (2), U_0 is the settling velocity for an isolated sphere, ε is the fractional liquid volume and $f(\varepsilon)$ is a function almost constant for ε ranging between 0.3 and 0.7, and is equal to 0.123.

According to Eq. (2), the constant settling velocity of multiple particles depends on the particle and resin characteristics only through the velocity term relative to the settling of a single particle. This means that the dependence of the constant settling velocity for multiple particles on these parameters is the same as in Eq. (1).

Ten years later, Richardson and Zaki (12) used a dimensional analysis to extract the relationship between the velocity of concentrated particles in a fluid and that of a single particle.

$$U = U_0 f\left(\varepsilon, \frac{D}{d}\right), \quad \text{with } d \text{ the settling tube diameter.}$$

By compiling experimental settling results from different authors and using some theoretical conclusions of Steinour, they obtained the following form for the function f: $f = \varepsilon^n$, with $n = 4.65 + 19.5\,D/d$ in the Stokes' flow regime.

For the study reported here, the particle size is very small compared to the internal diameter of the settling vessel, and the correction brought by Richardson and Zaki, which is the influence of the particle size on the ratio between the velocity of concentrated particles settling in a fluid and that of a unique particle, is negligible.

DISCUSSION

The similarity between the batch settling curves measured with our resin and displayed in Figs. 1–3, and the typical batch settling behavior obtained in waste treatment and metallurgical and chemical slurry thickening as shown in Fig. 4 is obvious. Due to the limited resolution determining mudline heights obtained by visual measurements, the compression regime was not resolvable and appeared as an horizontal line.

The Reynolds number was determined using the constant settling velocities corresponding to the zone-settling regime shown in Figs. 1–3. It ranged between 10^{-8} and 10^{-12}, depending on the temperature, the powder, and the resin formulation. This positions the particle settling in our resin system well into the Stokes' regime. In that case, Eq. (1) becomes

$$U_T = \left[\frac{gD^2(\rho_s - \rho)}{18\eta}\right] \tag{3}$$

The settling tests have been performed with our resin system varying some possible parameters of the settling process, the particle size and material, the temperature, and one of the resin components. In comparing the settling behavior of our resin system to the sedimentation model described by Eqs. (1) and (2), the constant settling velocities extracted from the slope of the first phase of the settling curves using a least squares fit (Origin software) are plotted as a function of the varying parameters. The error in the slope determination is represented as an uncertainty around each constant settling velocity data.

A first parameter is the particle diameter. Figure 5 displays the variation of the constant settling rate as a function of the PMMA particle diameter on a log–

log scale for the TEGDMA and the DEGDA resin formulations at room temperature (21°C). The two sets of data are following pretty well a square law, which indicates that the constant settling rate is proportional to the square of the particle diameter. This result is in accordance with Eq. (3).

Another parameter that has been varied is the temperature, which modifies the resin viscosity. The constant settling rates for the 40.5-μm P(MMA-*co*-EGDMA) particles in TEGDMA and DEGDA formulations plotted on a log–log scale as a function of the fluid viscosity are shown in Fig. 6. An acceptable fit by an allometric function can be obtained for the TEGDMA formulation with a power coefficient of -1.3, close to the inverse proportionality indicated in Eq. (3). The data are more scattered for the DEGDA formulation.

The characteristics of the resin affect both the density and the viscosity. According to Eq. (3), the constant settling rates plotted vs. $(\rho_s - \rho)/\eta$ should fall on a universal curve, linear with intercept at zero, for all resins with the same filler particles. Figure 7 displays the settling data for TEGDMA and DEGDA formulations with 40.5-μm P(MMA-*co*-EGDMA) particles as a function of $(\rho_s - \rho)/\eta$, showing an acceptable accordance with Eq. (3).

The last varied parameter is the particle material. Settling experiments have been performed with PMMA and P(MMA-*co*-EGDMA) particles. Unfortunately, these two materials have the same density. On the other hand, they behave very differently, and it was not possible to obtain powders of 5-μm PMMA particles. Constant settling rates for the $\sim$50-μm PMMA and P(MMA-*co*-EGDMA)

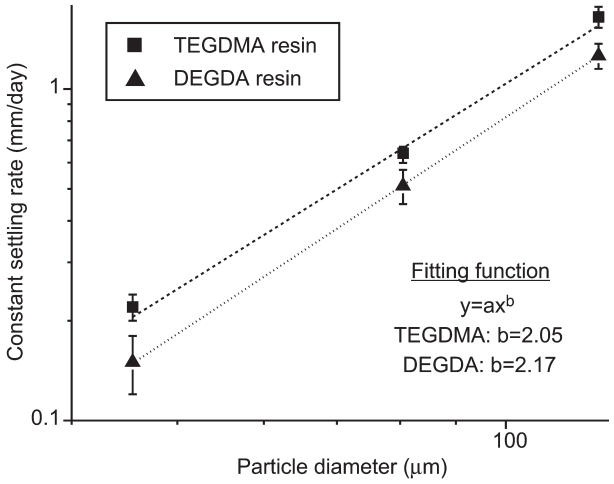

Figure 5. Constant settling rate as a function of the particle diameter, on a log–log plot, for PMMA filler settling in TEGDMA and DEGDA resins at 21°C.

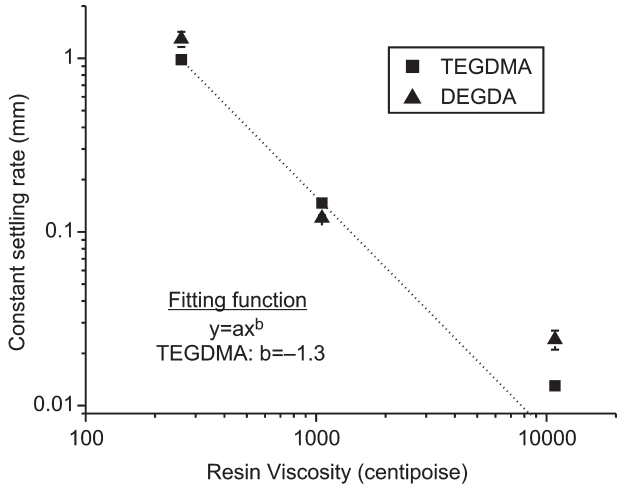

Figure 6. Constant settling rate as a function of the resin viscosity, on a log–log plot, for 40.5-μm P(MMA-*co*-EGDMA) particles settling in TEGDMA and DEGDA resins.

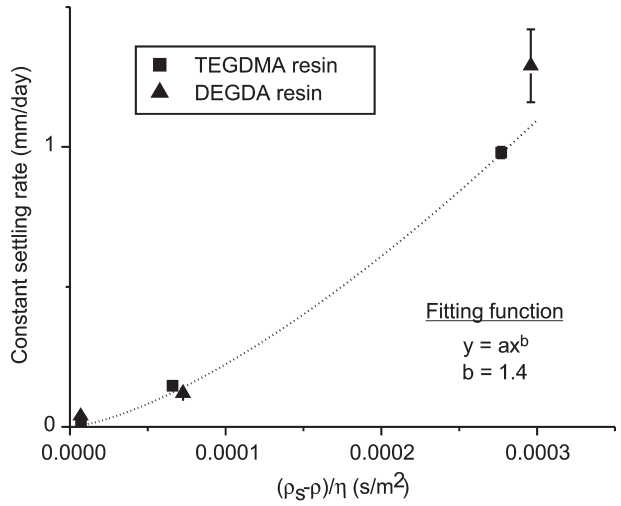

Figure 7. Constant settling rate as a function of the resin properties, for 40.5-μm P(MMA-*co*-EGDMA) particles in TEGDMA and DEGDA resins.

particles in TEGDMA and DEGDA resins at the three studied temperatures have been plotted side-by-side in Fig. 8. The settling rates are normalized by the square of the particle diameter (44.6 μm for PMMA and 40.5 μm for P(MMA-*co*-EGDMA)) to account for the small difference in the particle sizes. Settling rates obtained with PMMA and P(MMA-*co*-EGDMA) correspond pretty well, indicating that the particle material acts on sedimentation only through its density, as noted in Eq. (3).

We have seen that the simple model reported above describes successfully the effect of the sedimentation parameters on the first stage of the settling process, the zone settling regime, of two types of acrylic powders in two bis-GMA based reactive resins. On the other hand, the reactive character of the slurries manifests itself in the further steps of the sedimentation process. Indeed, we have found that the PMMA particles were more likely to react with the liquid fraction of the dispersion, leading to a more rapid onset of the transition regime and eventually to the full solidification of the resin in the settling vessel, as can be seen in Fig. 2. We attribute this phenomenon to a higher free radical concentration present on the PMMA particle surfaces than on the corresponding copolymeric particle surfaces. Higher radical concentrations could be the result of fractures arising

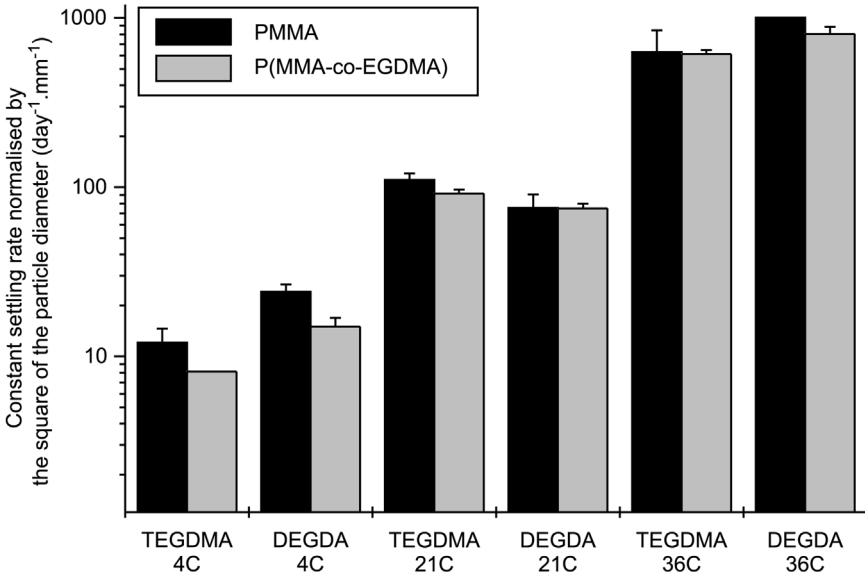

Figure 8. Constant settling rates in different conditions compared for the PMMA and the P(MMA-*co*-EGDMA) particles. The constant settling rate values are divided by the square of the particle diameter to take into account the effect of the size difference.

from particle grinding (13). Given that the viscosity of the resin will increase with the level of conversion of the monomer, the earlier demarcation to the transition regime would then be the result of a dynamic viscosity in the reactive fluid interacting with the particles.

This set of batch settling experiments have also revealed the limitations of visual mudline measurement, especially at the beginning of the settling process before clear separation appears between the supernatant fluid and the rest of the system, when the settling process is very slow, and in the compression regime. The limitations are even more obvious when no clear mudline is observed. For that purpose, a *z*-axis translating laser light scattering device (14) has been designed to allow the extraction of the particle concentration in the fluid along the whole settling vessel length, enabling a clear picture of the settling behavior in the three regimes (zone, transition, and compression) (15).

CONCLUSION

Settling rates have been measured for slurries of acrylic particles in an acrylic resin system with varying the particle size and material, and the resin viscosity and material. The results have been compared to batch settling models developed for waste treatments and metallurgical and chemical thickening. A good agreement between the two was obtained for laminar flow conditions, i.e., in the Stokes' regime. This has allowed an analysis of the sensitivity of each of the test parameters on sedimentation. In particular, the constant settling rate, slope of the first part of the settling curve, is inversely proportional to the fluid viscosity, linear with the particle and resin density, and proportional to the square of the particle diameter.

This last result can be exploited to reduce the incidence of sedimentation on the shelf life of filled resins. By reducing the filler particle size, one can greatly reduce the occurrence of separation between resin and filler, and increase the shelf life of the filled resin. This effect has been verified with the study of the settling behavior of our resin systems filled with 5.1-μm P(MMA-*co*-EGDMA) particles. No settling has been visually observed over 4 months at room temperature, indicating a very slow phenomenon.

ACKNOWLEDGMENTS

The authors want to thank Jeff Schultz and Todd Heil for their help with the particle size measurement. This project has been founded by a contract with the U.S. Navy through A&T Corporation.

REFERENCES

1. Allen, J.R.L. *Physical Processes of Sedimentation: An Introduction*; Allen and Unwin: London, 1970.
2. Pearse, M.J. Theories of Sedimentation. *Gravity Thickening Theories: A Review*; Warren Spring Laboratory: Stevenage, 1977; 11–17.
3. Papanicolaou, A.N. Settling Characteristics of Particles in a Suspension of Medium to High Solids Concentration. Master Thesis, Virginia Polytechnic Institute and State University, Blacksburg, VA, USA, 1992; 1–13.
4. Bowen, R.L. Properties of a Silica-Reinforced Polymer for Dental Restorations. J. Am. Dent. Assoc. **1963**, *66*, 71–78.
5. Htang, A.; Ohsawa, M.; Matsumoto, H. Fatigue Resistance of Composite Restorations—Effect of Filler Content. Dent. Mat. **1995**, *11* (1), 7–13.
6. Condon, J.R.; Ferracane, J.L. In Vitro Wear of Composite with Varied Cure, Filler Level, and Filler Treatment. J. Dent. Res. **1997**, *76* (7), 1405–1411.
7. Dolez, P.; Marek, M.; Love, B.J. Photopolymerizable Acrylic Resin: Effect of the Curing Time and Temperature. J. Appl. Polym. Sci. **2001**, *82*, 546–554.
8. Love, B.; Kuhr, T.; Holton, C.; Grant, J.W.; Courson, B.; Claus, R. Light Cured Adhesive. US Patent Application 09/340,052, June 29, 1998.
9. Dolez, P.; Love, B.; Holton, C. Hydrophilic Photocurable Adhesive for Marine Applications. Patent Disclosure, Virginia Tech Intellectual Properties VTIP 00-121, August 3, 2000.
10. Weber, W.J., Jr. Sedimentation. *Physicochemical Processes For Water Quality Control*; Wiley: New York, 1972; 111–115.
11. Steinour, H.M. Rate of Sedimentation, Nonfloculated Suspensions of Uniform Spheres. Ind. Eng. Chem. **1944**, *36*, 618–624.
12. Richardson, J.F.; Zaki, W.N. Sedimentation and Fluidisation: Part I. Trans. Inst. Chem. Eng. (London) **1954**, *32*, 35–53.
13. Kausch, H.H. Identification of ESR Spectra of Mechanically Formed Free Radicals. *Polymer Fracture*; Springer-Verlag: Berlin, Heidelberg, 1987; 141–163.
14. Hoffman, D.L.; Brooks, D.R.; Love, B.J. Settling Device. Patent Disclosure, Virginia Tech Intellectual Properties VTIP 01-091, August 22, 2001.
15. Hoffman, D.L.; Brooks, D.R.; Dolez, P.I.; Love, B.J. Design of a *z*-axis Translating Laser Light Scattering Device for Particulate Settling in Dispersed Fluids. Submitted to Rev. Sci. Instr.

Received May 2001
Revised November 2001